



VTOL analysis for an agile fixed-wing UAV

AENG30017

Research Project 3

Aerospace Department

Joaquim Bolós Fernández

jb17029

March, 2020

Mitigation Plan

Event/Issue	Potential/Actual impact on the Project	Action(s) taken to mitigate impact on project outcomes	Remaining Impact
Experimental flight testing for the improved BUDDI configuration couldn't be conducted.	Key aspect of the project was to compare original BUDDI performance with the proposed configuration with the data and parameters extracted in initial analysis.	The scope of the project was changed from validating the improved BUDDI configuration experimentally, to a more in-depth study on how to improve the current configuration in terms of pitch response.	Proposed configuration hasn't been validated. Therefore, comparison with current configurations could prove the changes implemented to worsen the performance.
No access to Bristol Flight Laboratory, so BUDDI Centre of Gravity (CG) was not determined.	For the Stability Analysis the current location of the centre of gravity, thus the initial static margin is unknown. Therefore, degree of reduction in static margin can not be accurately calculated.	Based on existing data, centre of gravity is assumed to be within 20 and 30 % of the Mean Aerodynamic Chord (MAC) and CG is shifted backwards along the longitudinal axis from 30% MAC onwards.	Precise location of CG is estimated, so final static margin reduction is not exact.

1 Executive Summary

In recent years, the use of drone technology, for investigation and remote monitoring, has been proved a resourceful technique worldwide, as it permits exploring without risking human lives. However, when investigations are conducted in hazardous environments, landing can be difficult due to the uneven ground or reduced landing areas presented, if there is any. Within all the wide variety of drones, agile UAVs, use recovery methods such as vertical landing[1], net recovery[2][3], arresting line recovery, skyhook recovery and para-sail, among others, to ensure a safe landing and retrieval of the aircraft. This type of drones are lightweight aircraft with big control surfaces, typically characterised by high thrust-to-weight ratios (2-3) and strong propwash [4]. In this project, the agile UAV being investigated - BUDDI (see Figure 1) - has been built by the University of Bristol Flight Lab to perform geological investigations on the volcano FUEGO (Guatemala). This environment presents rocky and uneven grounds and it is thus unsafe for conventional landing. This drone, in particular, is capable of vertically take-off and landing, which is convenient, as additional structures are not required to recover or launch it.



Figure 1: BUDDI CAD model produced by Thomas David,
University of Bristol

The aim of this research project is to effectively present a better configuration for BUDDI with respect to its vertical take-off and landing (VTOL) capabilities and thus, its mission performance. Both take-off and landing are high power consuming phases of the mission. Consequently, reducing the duration of the manoeuvres and increasing their efficiency is key to extend battery life and analogous investigation.

Performance analysis of the current configuration

In order to asses VTOL capabilities, a criterion needs to be established. Therefore, an initial analysis of the current configuration is carried out to extract key parameters from the current configuration for future comparison with potential enhanced configurations. The analysis is divided into 4 steps:

Data Gathering from Experimental Flight Testing: An initial flight test simulating the mission to be carried out during FUEGO investigation is conducted to gather experimental data. The mission flight plan consists of vertically taking off from the base, flying above the volcano - for scientific data gathering and ash collection -, and finally, from hover, vertically descend and land on the base.

Data Processing: The raw data extracted from testing requires transformations of units and values in order to be usable. Therefore, a Matlab Code is developed to interpret the data, modify it if needed, and finally used to obtain figures or values of interest that essentially show the drone behaviour and status.

Phase Separation: During the experimental testing, data is gathered for the whole flight test. However, only vertical take-off and landing will be looked in detail. Take-off is considered a phase itself, but landing is divided in 3 phases: transition into hover, hover and transition out of hover. Consequently, the code developed extracts only data from phases of interest, which are determined according to the pitch and airspeed. Both variables accurately represent the transition from vertical steady position to forward horizontal flight at cruise speed and the other way around.

Phase Analysis: For each individual phase, a different analysis is conducted and only specific relevant data will be taken into account to asses its performance. Potentially, after the analysis, a series of parameters and phase characterisations are determined to allow comparison between future configurations and present model. The analysis is presented below:

1. Take-off

This manoeuvre (see Figure 2) proved to rely on a throttle impulse to launch the drone and a later elevator input to transition from vertical position to horizontal forward flight. The time to perform the manoeuvre was found to be 6.4 seconds, and the current consumption 6.46×10^{-6} amps/ μ s. In addition, pitch transition was observed to had a disturbance due to the sudden elevator input, and a mean absolute error of the manoeuvre with respect to an ideal transition in pitch was found to be 12.48%.

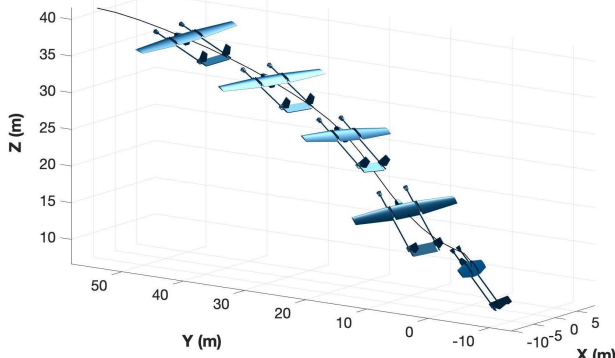


Figure 2: Take-off trajectory

than in manual transition (3.85×10^{-6} amps/ μ s).

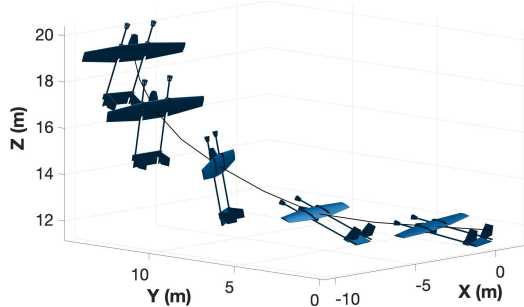


Figure 3: Transition into the hover trajectory

2. Transition into the hover

For this particular phase, represented in Figure 3, a separate analysis is carried out for a manual transition (executed through pilot commands), and an automatic transition (performed by the controller in a specific flight mode). The manual transition was observed to be faster (0.7 seconds), whereas the auto transition (4.7 seconds) was more stable and smoother. As in take-off, manual mode relied on a sudden increase in throttle and elevator input, which would give a faster but highly non-linear transition in terms of pitch. On the other hand, the throttle was off and pitch increased gradually for the auto transition. Consequently, current consumption in auto (1.29×10^{-6} amps/ μ s) was lower

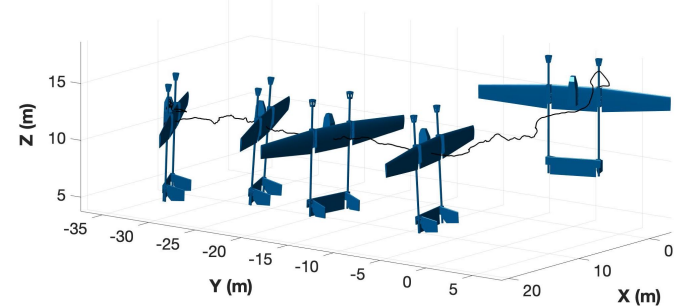


Figure 4: Hover Trajectory

3. Hover

In the hover, control authority was overlooked, and a different analysis approach was taken to asses the ability to hold pitch angle and vertical position. Firstly, an mean absolute error of 3.47% was calculated of pitch with respect to a constant pitch of 90 degrees. Secondly, Z position appeared to fluctuate within ± 1 meter with throttle at the 25% of its full capacity. Finally, due to the extra throttle input to prop-hang, the current consumption (4.13×10^{-6} amps/ μ s) proved to be relatively high.

4. Transition out of the hover

Finally, vertical transition out of the hover (Figure 5) proved to be fast with time elapsed of 3.4 seconds. However, current consumption (7.76×10^{-6}

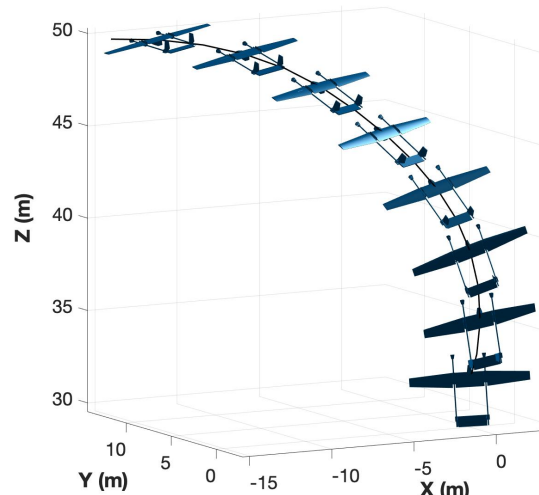


Figure 5: Transition out of the Hover

amps/ μ s) was the highest, as this phase has to compensate for the boost in both kinetic and potential energy. In terms of control, authority remained high as elevator was slightly actuated, and pitch transition only introduced subtle disturbances after achieving horizontal state.

Modifications to BUDDI Configuration

After performing the initial analysis of the current configuration, modifications to BUDDI configuration are proposed in order to enhance its VTOL capabilities improving its pitch response. The objective is to achieve a faster but still stable transition in and out of the hover. Consequently, the variation of the CG along the longitudinal axis and possible modifications to the code running on the controller (firmware) are both investigated as a means to achieve a better performance.

The centre of gravity - assumed to be within the 20-30% of the Mean Aerodynamic Chord - is shifted backwards on the longitudinal axis to reduce Static Margin. This gives a less stable aircraft with a higher pitch response. Furthermore, a stability analysis is conducted in XFLR5 to asses at what extent the variation of CG can make BUDDI unstable. Table 1 shows the stability analysis results.

CG Position(m)	MAC(%)	Static Margin (m)	Slope
0.044	25	0.078	-0.439
0.048	27.5	0.074	-0.419
0.053	30	0.069	-0.389
0.076	43.25	0.046	-0.259
0.099	56.25	0.023	-0.124
0.122	69.3	0	0

Table 1: Extracted parameters from transition into Hover

Finally, no actual changes in firmware are set in the new configuration, as a new transition script would need to be validated through simulation first. However, a proposal in firmware default parameters is presented for future investigation.

In the end, criteria to asses VTOL capacities is provided. The Matlab code developed and data processing for the investigation proved to be functional, thus key parameters were determined to allow comparison with potentially improved BUDDI configurations. Current configuration demonstrated a good pitch response, as pitch matched the elevator input, and lag between them was relatively low. However, the proposed configuration aims to increase the sensitivity of pitch with respect to the elevator deflection through a reduction in static margin, so lag is reduced further. Consequently, the next natural step in this research would be to test the potentially improved BUDDI configuration and compare the data obtained with the current one.

Analysis method could then be improved, so the code automatically detects the phases of interest based on flight mode, pitch angle, airspeed and altitude. Furthermore, more investigation could be done so data transformation allows analysis for other aircraft based on static margin.

In terms of improving the pitch response, physical modifications like: increasing the elevator, providing BUDDI with faster actuators and reducing mass distribution, could be investigated. However, all these modifications would also require an analysis of how they would affect the stability of BUDDI. Therefore, a more accurate aerodynamic model of BUDDI with the included body and spars could be used.

Ultimately, in the long term, high precision non-linear controllers and other control approaches may be implemented in order to better deal with the highly non-linear aerobatics endured by BUDDI. Furthermore, the corresponding simulation of their response could be investigated too in order to reduce the risk in experimental flight testing.

2 Introduction

The use of drone technology, otherwise known as Remotely Piloted Aircraft Systems (RPAS), for investigation and remote monitoring, has been proved a resourceful technique worldwide, as it does not require humans on-board and permits investigation without risking human lives. However, investigations in hazardous environments, usually involve terrains which will difficult or even prevent the landing, as uneven grounds, reduced landing areas or no landing ground at all. Sophisticated and Military Unmanned Aerial Vehicles (UAV) can avoid this issue by having a remote base structure as a launching and landing point [4], but simpler models, such as agile UAVs, precise other recovery methods to ensure a safe landing and retrieval of the aircraft.

This project, initially investigates different recovery methods for agile UAVs, assessing their strengths and capabilities. Then, after devising some criteria the vertical landing method is developed, performed and analysed. After the analysis, a new configuration is presented to achieve better performance in vertical take-off and landing.

The drone being investigated - BUDDI (Figure 6) - has been built by the University of Bristol Flight Lab. The goal of the said drone is to perform geological investigations on the volcano FUEGO (Guatemala), which presents rocky and uneven grounds and is thus unsafe for usual landing.



Figure 6: BUDDI CAD model produced by Thomas David, University of Bristol

3 Background

Since UAV's technology emerged, different methods to recover agile UAVs have been tested, as they are versatile, affordable and their applications and use is widespread.

A few methods of recovery are based on typical aircraft landing methods, like runaway landing or vertical landing. However, with their reduced weight and size, non-conventional methods such as recovery by parachute, deep stall, windsocks, skyhook, nets or wires are also feasible. With these methods when the drone impacts with the ground or landing structure - like a net - at a relatively low speed, the aircraft damage is - in most cases - negligible.

Broader research has been conducted on non-conventional landing methods, for example, Nets recovery with vision-based automatic landing [2] on a fixed structure, or on a mobile ground vehicle with a structure mounted on it [3]. Nevertheless, research has also been conducted for methods like vertical and deep stall landing, which strongly rely on the manoeuvrability of the drone itself and its ability to perform the aerobatics required to land. Thus, research on these methods focuses on control for Agile UAVs [5][1].

Control methods and dynamics modelling for this kind of drone constitute part of a broader research topic that not only focuses on landing methods, but in manoeuvrability, the aerobatic performance of the aircraft, and automating the performance itself. In Dr Waqas Khan's thesis and its derived conference

paper [6, 7], it is described how to model dynamics for UAV through first principles. That meaning, that physical effects are modelled from theoretical assumptions rather than with flight test data for identification. The latter generally tends to result in a more accurate control model, at the expense of exhaustive wind tunnel testing. Previous similar studies from MIT [8] had been conducted to generally describe the nonlinear dynamics from first principles too, but the presented model is not as complete as Khan's, as it lacks thruster dynamics and propeller slipstream effects.

As mentioned above, automating the manoeuvres is part of control methods studies, so the following studies are conducted once the dynamics of the aircraft are established. Following Khan's dynamics modelling, an autonomous control system for an agile fixed UAV is presented in [9]. This single control system is capable of a wide variety of aerobatic manoeuvres, and demonstrates knife/edge, rolling harrier, hover, aggressive turnaround and transition between these manoeuvres. An in-depth study of hover using an alternative control system is presented in [10]. Both control models aim to control position and orientation. In addition, it can be seen that in order to avoid Gimbal Lock - an event likely to happen due to aerobatics included in the flight envelope - attitude is represented with quaternion rather than with Euler Angles in both control models.

Simulation environments are highly resourceful when it comes to proving the correct functioning of the system before real-life testing. Further studies [11] implement manoeuvres previously mentioned [9] in a Hardware-in-the-Loop (HIL) simulation environment, and later, in flight testing. Therefore, the control system can be validated and proved to be functional to perform the aerobatics automatically.

In this project, the control system integrated into BUDDI is already capable to perform hover, so the control method is valid and ready to perform the aerobatic manoeuvre . Therefore, in this project, the performance of the controller during vertical take-off and landing is evaluated and suggestions for future development are presented.

4 Aims, Objectives and Technical Methodology

The aim of this research project is to effectively present a better configuration for BUDDI with respect to its vertical take-off and landing (VTOL) capabilities and thus, its mission performance. Both take-off and landing are high power consuming phases of the mission. Consequently, reducing the duration of the manoeuvres and increasing their efficiency is key to extend battery life and analogous investigation.

The project breaks down in 2 objectives:

1 Performance analysis of the current configuration: A criterion needs to be devised when it comes to asses vertical landing and mission capability. Therefore, the analysis extracts key parameters from the current configuration for future comparison.

- **Data Gathering from Experimental Flight Testing:** An initial flight test simulating the mission is performed in the Farm House Facility (Figure 7) by the pilot Thomas David, a PhD student from the University of Bristol. BUDDI's mission plan to be carried out during FUEGO investigation consists on vertically taking off from the base, flying above the volcano - for scientific data gathering and ash collection -, and finally, from hover, vertically descend and land on the base. Therefore, during the flight test, mission phases are recreated and experimental data from the drone during the take-off, flight path, transition in and out of the hover, and hover itself is gathered. The data collection process is described in section 5.1 and data used for the analysis is detailed in Figure 9.



Figure 7: BUDDI Flight Testing in Farm House Facility - University of Bristol

- **Data Processing:** The data requires transformations of units and values in order to be usable. Therefore, a Matlab Code is developed to interpret the data, modify it if needed, and finally used to obtain figures or values of interest, that essentially show the drone behaviour and status. In addition, code iterates only through selected time periods, those being either the whole flight or selected phases. This process is also detailed in section 5.1.
- **Phase Separation:** During the experimental testing, data is gathered for the whole flight test. However, only vertical take-off, transition into hover, hover and transition out of hover will be looked in detail. The analysis of those particular phases is key to get a better understanding of the aerobatic capabilities of BUDDI among others.

The vertical take-off performance is of interest, firstly, because it is the initial flight phase - so the success of the rest of the mission depends on it -; and secondly because it can provide an insight of the pitch response of the aircraft. Parameters such as time elapsed to transition to forward flight, battery consumption, pitch response and control authority, are considered when devising criteria to establish which take-off manoeuvre is best. On the other hand, transition into the hover, hover and transition out of the hover are exclusively used to analyze the landing performance. The vertical landing manoeuvre is the main focus of this research project, so it is of interest to asses how the transition into hover is carried out, how well the drone keeps the position in hover - as the descend in hover needs to be as smooth as possible and be kept within the landing area boundaries -, and how would the drone transition out of the hover in case that the landing needs to be aborted.

Consequently, during the data analysis, the code focuses the attention on data from the relevant phases of the mission, which are determined according to the pitch and airspeed. Both variables accurately represent the transition from vertical steady position to forward horizontal flight at cruise speed and the other way around. Furthermore, Mode of BUDDI is investigated to determine hover time period - as when the aircraft is hovering is in Q-MODE - and distinguish between a manual and an auto transition into the hover (as an automatic transition is triggered when its corresponding mode is switched on).

- **Phase Analysis:** For each phase a different analysis is conducted and only specific relevant data will be taken into account, to asses their performance. For all sections, the time elapsed and battery consumption are examined. Other main insights researched are a comparison of experimental versus ideal pitch during take-off and hover, the effect of climb on battery used during transitions, and variation of height while hovering. Potentially, after the analysis, a series of parameters and phase characterisations are determined to allow comparison between future configurations and current one.

The analysis is detailed in section 5.2

- 2 Modifications to BUDDI Configuration:** After performing the initial analysis of the current configuration, modifications to BUDDI configuration are proposed to enhance its landing capabilities improving its pitch response. In other words, achieving a faster, but still stable transition into the hover.

The centre of gravity (CG) is shifted backwards on the longitudinal axis, reducing static margin, which gives a less stable aircraft with a higher pitch response - which potentially leads to a faster transition into hover -. However, a stability analysis is conducted to asses at what extent the variation of CG can make

BUDDI unstable. Ultimately, the code running on the controller (firmware) is analyzed and potentially customized to improve the transition into hover. Details of the proposed changes are explained in section 5.3.

5 Scientific studies

This section presents the research activity detailed in section 4.

5.1 Data Gathering and Processing

The controller of the Drone is contained into the Pixhawk unit (Figure 8), a piece of hardware supported by ArduPilot, that provides the controller with customized navigation software (firmware). This unit contains peripheral sensors such as gyroscopes, magnetometer and barometer, and can output signals to ESC's, servos and rotors (among other devices) that all put together act as the vehicle's eyes, brain and motive unit.

For the data gathering, a micro SD card is incorporated into the Pixhawk unit so readings from sensors are all recorded. Then, after the experimental flight, the drone is connected to a ground station (PC) and through Mission Planner (ArduPilot Software) the .bin file that contains all the flight data is converted into a .mat file so Matlab can interpret the data of the mission log.

Log data is organized in a structure of matrices. The matrices used in the Matlab code that contain the parameters of interest are described in Figure 9.



Figure 8: Unmanned Hawk PX1 32 bit Unit

GPS (Global Positioning System)

Lat	Latitude according to GPS (deg)
Lng	Longitude according to GPS (deg)
Alt	GPS reported altitude (m)

ARSP

Airspeed	Airspeed recorded from pitot tube (m/s)
----------	---

MODE (Flight Mode)

Mode	Flight Mode: Manual(0) - Transition (10) - Hover(18)
------	--

ATT (Attitude information)

Pitch	The vehicle's actual pitch angle in degrees (pitch forward is negative, pitch back is positive)
Roll	The vehicle's actual roll in degrees (roll left is negative, right is positive)
Yaw	The vehicle's actual heading in degrees with 0 = north

AETR (Control Surfaces information)

Ail	Ailerons deflection (from -4500 to 4500)
Elev	Elevator deflection (from -4500 to 4500)
Thr	Throttle (from 0 to 100)
Rudd	Rudder deflection (from -4500 to 4500)

IMU (Inertial Measurement Unit: Accelerometer and gyro data)

GyrX,GyrY,GyrZ	The raw gyro rotation rates (Pitch, Roll and Yaw rates) in degrees/second
AccX,AccY,AccZ	The raw accelerometer values in m/s^2

BAT (Battery Data)

Curr	Instant current drawn from battery in amps
CurrTot	Total current drawn from battery in amps

Figure 9: Data matrices used for analysis

However, to analyse the data, some transformation of units and values need to be applied.

Firstly, for clarification in BUDDI's location, Latitude and Longitude values (transformed to radians) are converted into meters using equation (1) and (2). Also, for ease of plot understanding, initial position vector (X, Y) is subtracted to all the other Cartesian coordinates to set an origin in the map.

$$X = R \times \cos(Lat) \times \cos(Lng) \quad (1)$$

$$Y = R \times \cos(Lat) \times \sin(Lng) \quad (2)$$

Secondly, in order to obtain a more intuitive value for control surfaces deflection - as specified in Figure 9 values vary approximately from -4500 to 4500 -, an indoor experimental test is performed to obtain the angle of deflection of the ailerons, rudders and elevator. During the test, the maximum deflections were measured in degrees for all control surfaces. Then, BUDDI was turned on and control surfaces were saturated so they would cause the maximum positive and negative pitching, roll and yaw moments (see Figure 10). From the data log obtained, a linear relationship can be established between maximum

values recorded in the ± 4500 domain (see Table 2), with the measured angles for each control surface to obtain deflection in degrees.

Finally, when the drone goes into the hover, Q-Hover mode is activated, which gives rise to a -90 degrees error in pitch readings due to the rotation of the reference body axis in Q-Hover. Therefore, code is designed to detect the error and correct it.

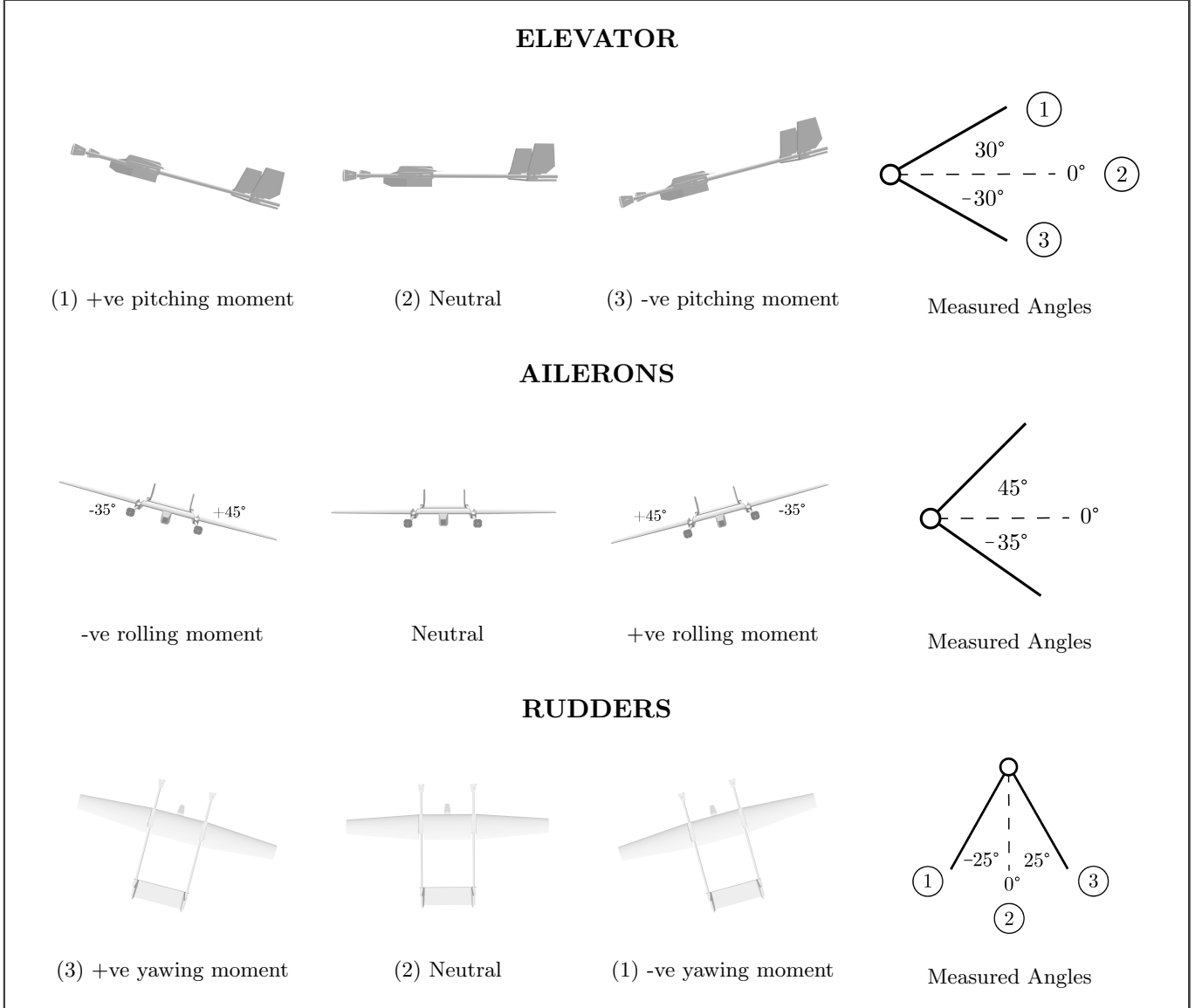


Figure 10: Measured angles deflection for all control surfaces

	Positive Moment		Neutral Moment		Negative Moment	
	PX1 Domain	Degrees	PX1 Domain	Degrees	PX1 Domain	Degrees
Elevator(δ_E)	4427	30	-275	0	-4500	-30
Right Aileron(δ_{AR})	-4429	45	72	0	4500	-35
Left Aileron(δ_{AL})	-4429	-35	72	0	4500	45
Rudders(δ_R)	4500	25	-17	0	-4500	-25

Table 2: AETR values for maximum deflection of control surfaces giving positive or negative moment

5.2 Phase Analysis

5.2.1 Take-off

The take-off manoeuvre starts off with BUDDI in a vertical position and launches with a throttle impulse. Once the drone is airborne, the elevator is used to transition from vertical position to horizontal forward flight. The take-off manoeuvre is physically represented in Figure 11.

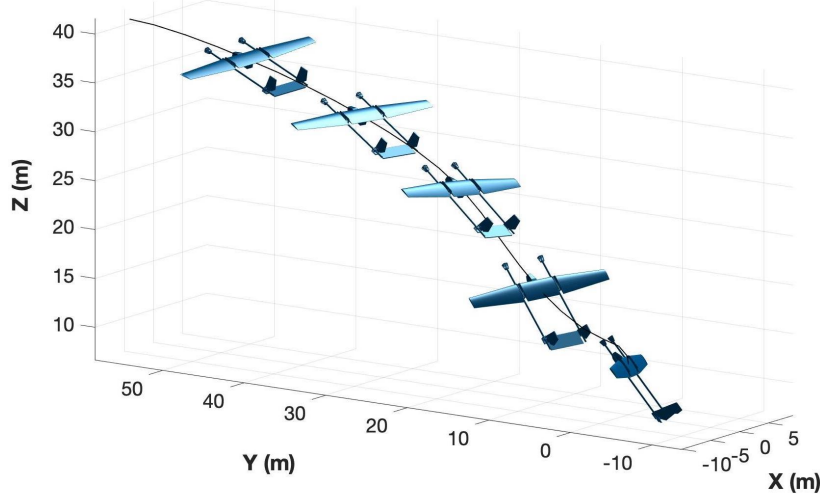


Figure 11: Take-off trajectory

As it can be seen in Figure 12, in terms of attitude, the drone rolls before being airborne, producing a brief disturbance in roll, which is paired with yaw by the sensors - as the drone is standing in a vertical position and sensors use an earth fixed reference-. In addition, at the very beginning of the take-off, a brief disturbance is introduced in pitch, which is soon corrected.

From Figure 12 time period to perform the manoeuvre is extracted (6.4 seconds) and a mean absolute error relating ideal and actual pitch response is calculated (MAE = 12.4825%).

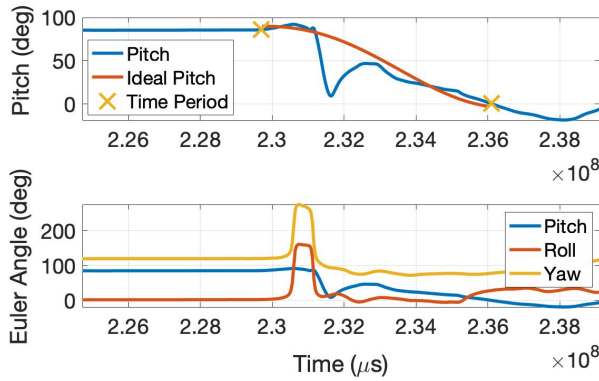


Figure 12: BUDDI's attitude during take-off manoeuvre

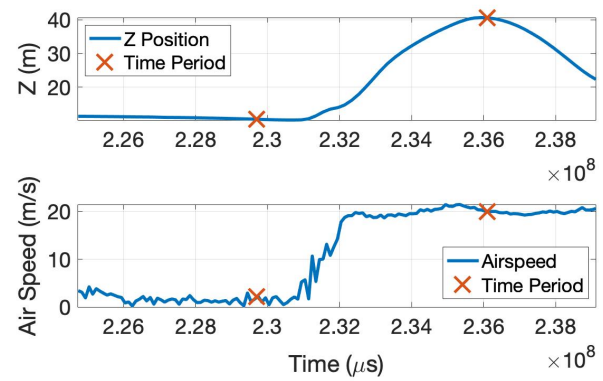


Figure 13: Airspeed and Z position vs time during take-off

From Figure 13, climb (30.11 m) and cruise airspeed (20 m/s) are obtained. Then, in Figure 14 it can be observed how pitch is influenced by a negative deflection of the elevator. Control authority (availability of control surface deflection) is almost saturated for a brief instant to introduce the trajectory. However, after the brief variation in elevator deflection, authority is recovered.

The throttle is saturated to initially lift BUDDI from the ground. Then, gradually decreases until the right amount to sustain flight regime.

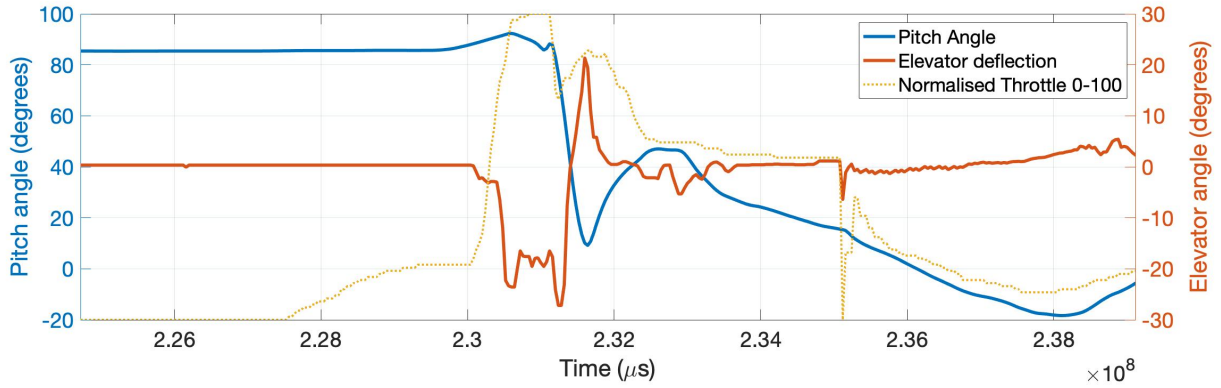


Figure 14: Pitch control authority in take-off

Current drawn from take-off (41.38 amps) can be extracted from Figure 15, settling the manoeuvre current consumption at 6.46×10^{-6} amps/ μs .

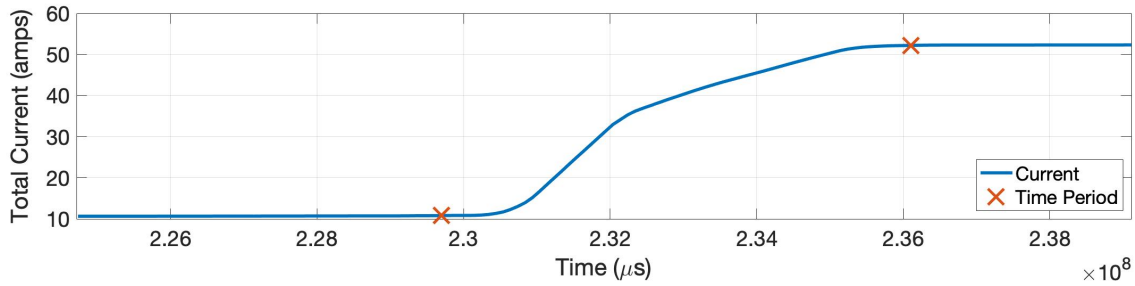


Figure 15: Total current drawn vs time

5.2.2 Transition Into Hover

In this section transition into hover is analyzed for manual transition (executed through pilot commands) and automatic transition (performed by an Ardupilot flight mode).

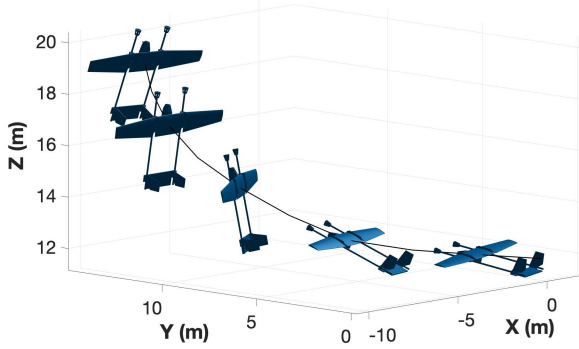


Figure 16: Manual transition into hover trajectory

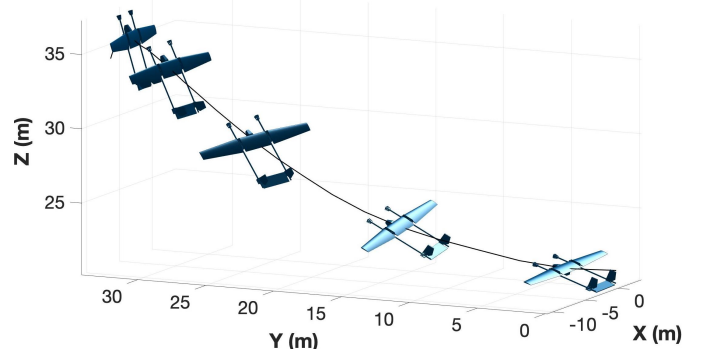


Figure 17: Auto transition into hover trajectory

As seen on Figures 16 and 17, both transitions successfully achieve hovering state. However, readings differ:

Manual transition (0.7 seconds) is much quicker than the auto transition (4.7 seconds), but it is also highly non-linear (see Figure 18) in pitch. The fact that the pitch is so sudden, makes BUDDI heavily vary in pitch, giving a rather prolonged oscillatory motion before settling at 90 degrees. In addition, a roll step input is generated right after the transition (again, coupled with yaw as the drone is in vertical position).

The auto transition manoeuvre is planned out by the controller to achieve a smoother transition into the hover state. The time elapsed to transition is higher and disturbances in pitch are not as significant as for manual transition. Looking at the aircraft attitude in Figure 19, it can be seen that when the transition starts, while BUDDI is transitioning to vertical motion, yaw and roll introduce a coupled damped oscillatory motion, which grows smaller during the transition.

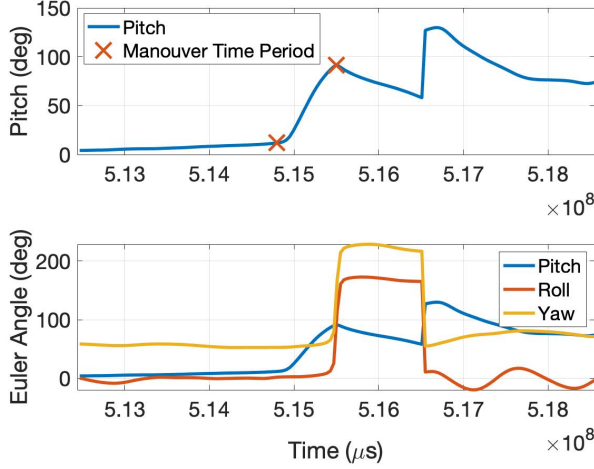


Figure 18: Attitude at manual transition

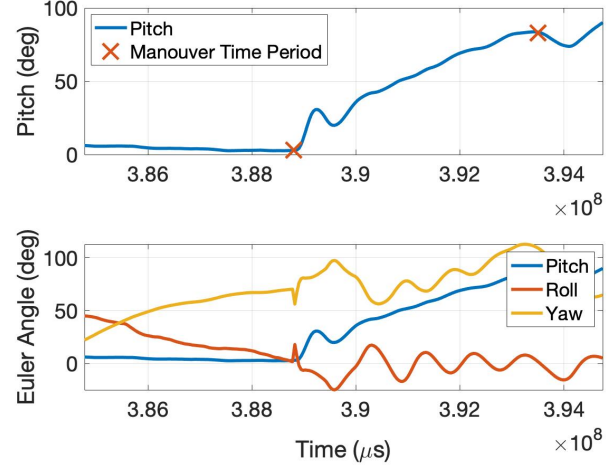


Figure 19: Attitude at auto transition

Climb and airspeed from both transitions can be extracted from Figures 20 and 21. In terms of altitude, climb in auto is higher during the transition (13.62 m). Nonetheless, during the manual transition, BUDDI increases height once it is already in vertical position. Even though climb during transition is small (2.16 m), it ends up escalating about the same height as the auto transition. In terms of airspeed, in both cases, transition reduces from cruise speed (≈ 20 m/s) to a speed of 2 m/s. Ideally, the Q-Hover airspeed would be zero. Nonetheless it fluctuates due to sensor noise.

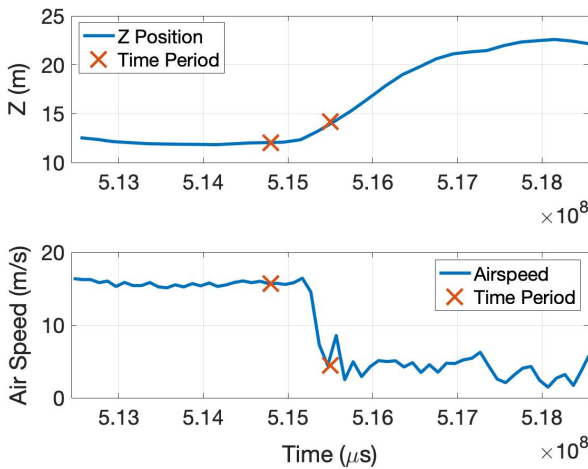


Figure 20: Airspeed and Z position vs time - Manual

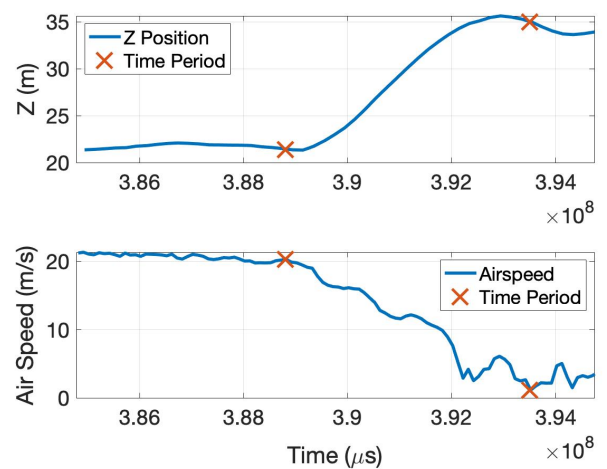


Figure 21: Airspeed and Z position vs time - Auto

In Figures 22 and 23, control authority in pitch can be observed:

The manual transition feeds a sudden step input to the elevator and gradually increases throttle up to 60% of its capacity. Consequently, elevator saturates at 30 degrees and aircraft climbs 2.16 meters until it reaches a vertical position. As soon as BUDDI achieves 90 degrees in pitch, the elevator deflection is pulled back to zero degrees and throttle capacity is reduced. Right after, the elevator keeps varying in order to correct later variations in pitch.

On the other hand, the auto transition introduces a slight sudden peak on elevator deflection, which is the cause of the disturbance in pitch, and is followed by a gradual deflection increase until BUDDI achieves hover. The control authority is not saturated at any time, as the maximum deflection during the

whole transition is about 20 degrees, and throttled is capped - which makes automatic transition better in terms of control -.

Finally, looking at Figures 24 and 25, it is noticeable that as the time elapsed is higher for the auto transition, so is the current drawn. This is due to the elevator being actuated for a higher period of time, even though the throttle is off during the auto transition. However, in terms of the current consumption with respect to time, the auto transition (3.85×10^{-6} amps/ μ s) is more efficient than the manual transition (1.29×10^{-6} amps/ μ s).

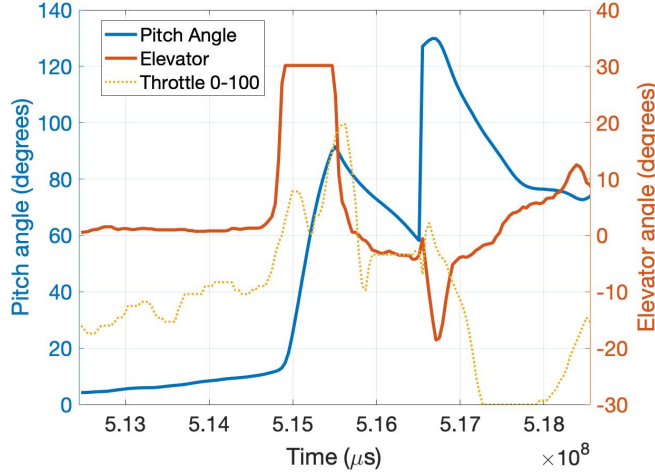


Figure 22: Pitch control authority - Manual

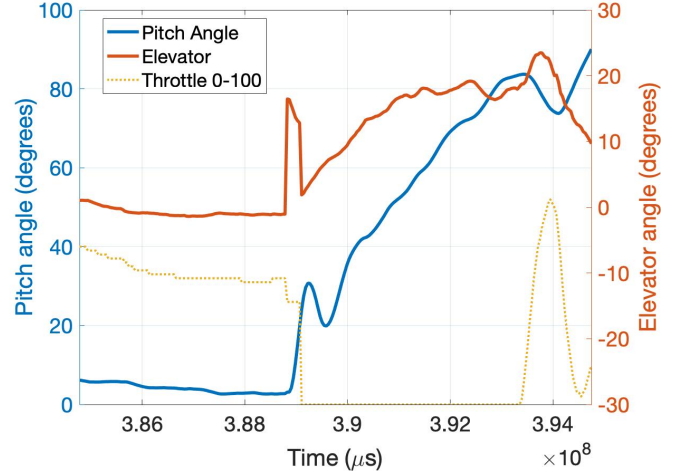


Figure 23: Pitch control authority - Auto

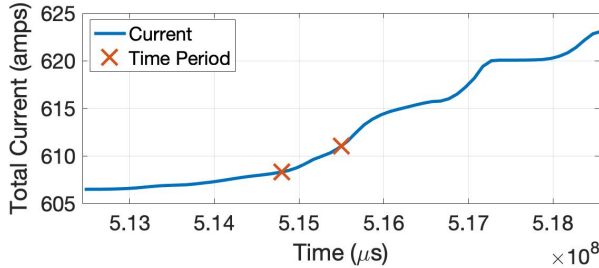


Figure 24: Total current vs time - Manual

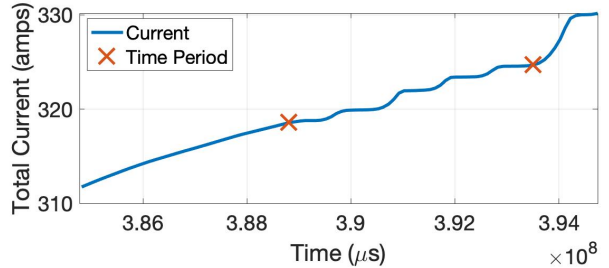


Figure 25: Total current vs time - Auto

	Manual Transition	Auto Transition
Time elapsed	0.7 s	4.7 s
Climb	2.16 m	13.62 m
Current drawn	2.7 amps	6.1 amps
Current Consumption	3.85×10^{-6} amps/ μ s	1.29×10^{-6} amps/ μ s

Table 3: Comparison between extracted parameters from manual and auto transition into the hover

5.2.3 Hover

In this section, BUDDI's hover performance is analyzed. Achieving this phase is fundamental in order to be able to perform a vertical landing. Therefore, as the transition to achieve the state has already been analysed, BUDDI's performance while holding hover is investigated.

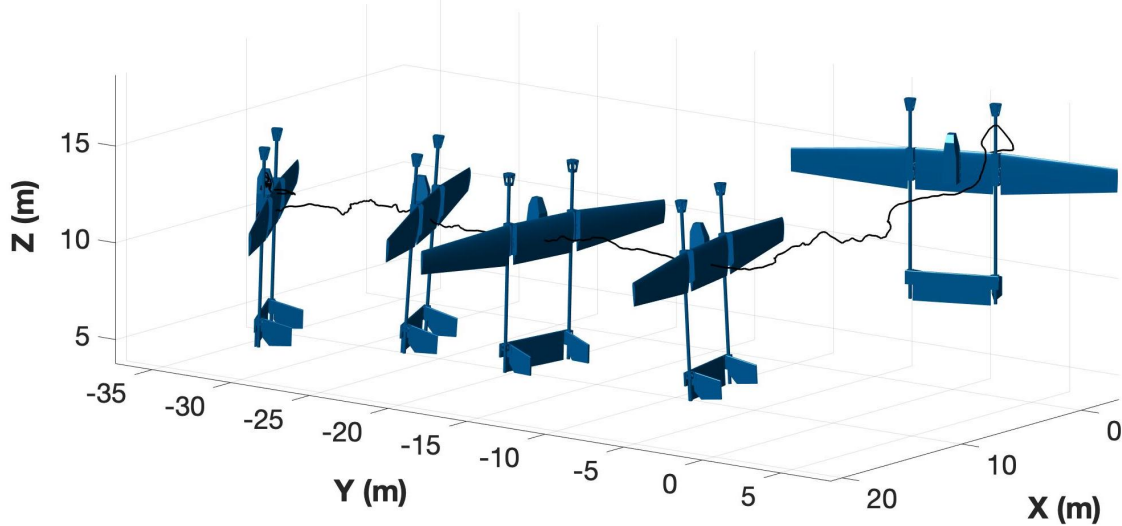


Figure 26: Hover trajectory

In Figure 26 hover trajectory is represented. It can be seen how BUDDI moves along the XY plane presenting roll motion. Looking closely at the attitude plot (Figure 27), at the beginning of the transition yaw and roll are paired, but as Q-Hover state is achieved, yaw is the only Euler angle that changes with time. Nonetheless, as mentioned above, what the aircraft is actually doing is varying in roll. The reason why this is misunderstood on sensors data is that readings from the magnetometer suggest a yawing motion along the Z earth axis. Therefore, yaw is read from an earth fixed frame rather than a body fixed frame.

Pitch slightly oscillates during the hovering period (74.5 seconds) giving a mean absolute error of 3.47% with respect to the 90 degrees assumed for vertical hover.

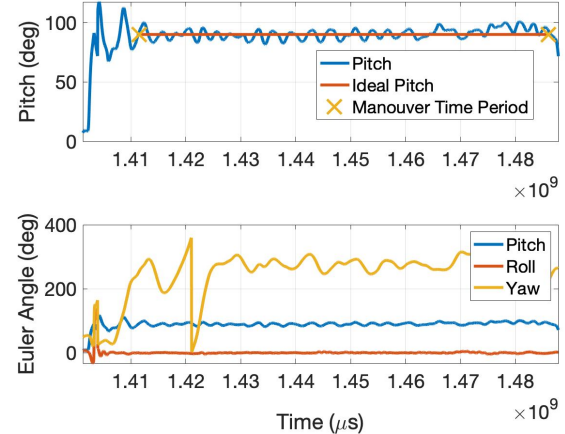


Figure 27: Attitude in hover

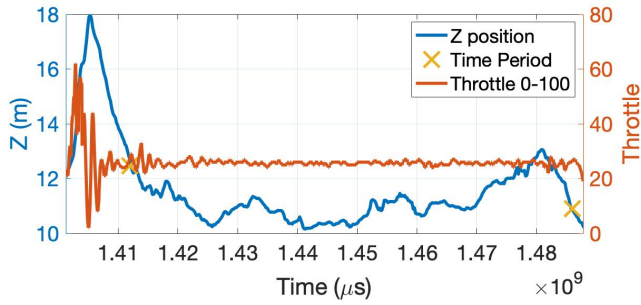


Figure 28: Z position variation with respect to Throttle

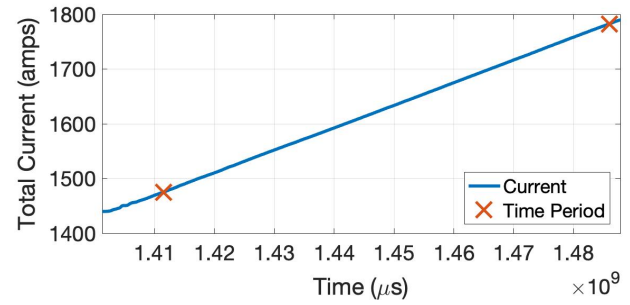


Figure 29: Current consumption during hover

Looking at Figure 28 it appears that even if the throttle input remains constant, Z position still fluctuates within ± 1 meter of its reference position.

Current drawn during this phase (307.5 amps - see Figure 29) is big due to the long time period of this phase. Furthermore, consumption with time is high (4.1275×10^{-6} amps/ μ s), meaning that sustaining hover is power demanding.

5.2.4 Transition Out of Hover

The transition out of hover (Figure 30) can be achieved in different ways, but in the experimental flight testing, throttle input is abruptly increased, making BUDDI climb straight and then recover horizontal flight. This particular manoeuvre choice is quite interesting, as its purpose would be to abort landing in case that something goes wrong, thus, the initial vertical climbing means a risk reduction in case there are any obstacles around.

The time taken to transition from hover to forward flight (3.4 seconds) can be extracted from Figures 31 and 32. In addition, BUDDI smoothly transitions from 90 to 0 degrees while climbing 19.75 meters, and gradually increasing airspeed until it meets cruise speed (≈ 20 m/s).

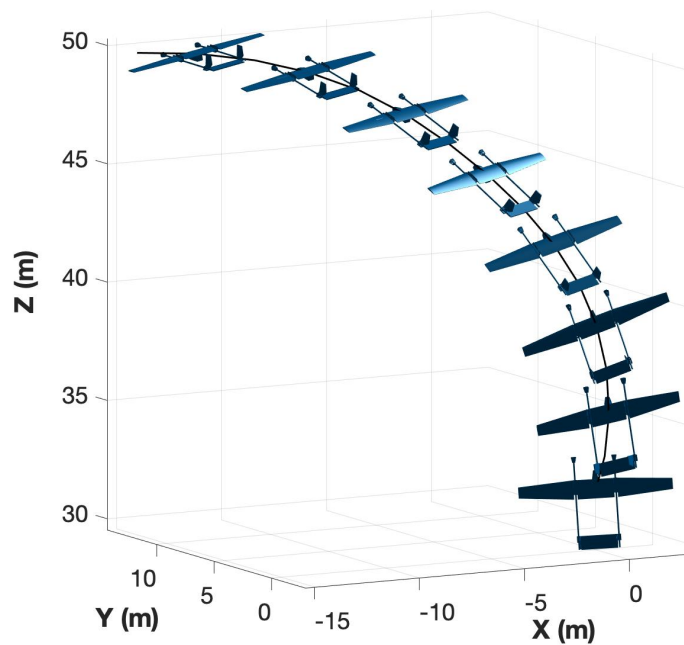


Figure 30: Transition out of hover trajectory

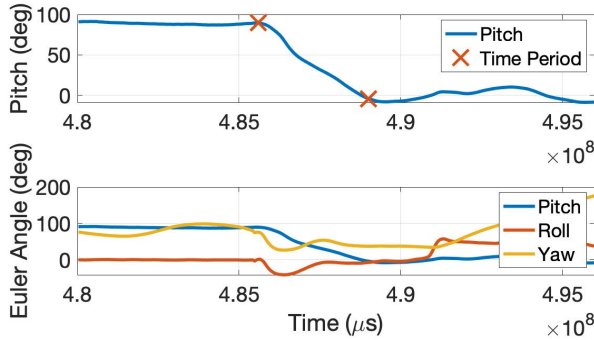


Figure 31: BUDDI's attitude during transition

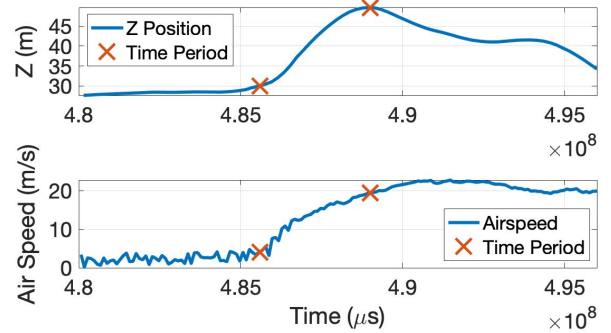


Figure 32: Airspeed and Z position vs time during transition

In terms of control, Figure 33 suggests that authority remains quite high, as only small elevator deflections are required to perform the manoeuvre. However, in order to lift the aircraft, the throttle is saturated and then gradually decreased until it reaches flight regime capacity ($\approx 20\%$). Consequently, when it comes to current consumption (26.4 amps - see Figure 34), the drone has to cover for loss in kinetic and potential energy, so current drawn with respect to time (7.76×10^{-6} amps/ μ s) is higher than in any other phase.

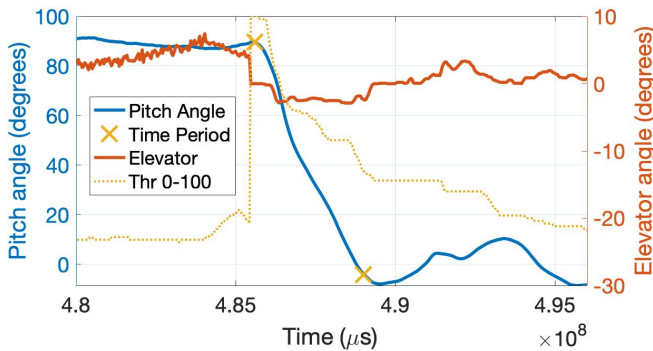


Figure 33: Control authority on pitch

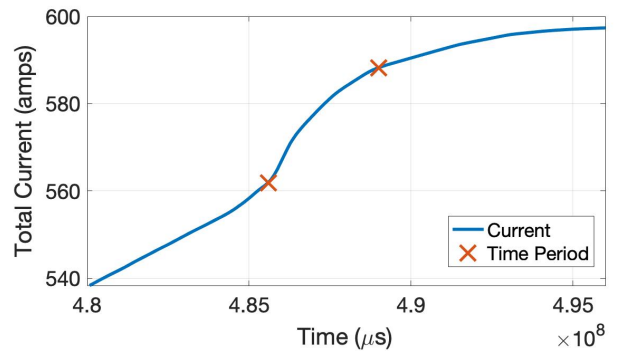


Figure 34: Total current drawn vs time

5.3 BUDDI Modification

Once the preliminary analysis has been conducted, modification in BUDDI focuses on how to transition faster into the hover through an increase in pitch response.

5.3.1 Centre of Gravity

As mentioned in methodology (Section 4), shifting the centre of gravity (CG) backwards along the longitudinal axis reduces the static margin (SM). Consequently, the aircraft is provided with a higher pitch response for a faster transition into the hover.

Computational Fluid Dynamics software (XFLR5) is used to determine the Neutral Point (NP) of the aircraft, the static margin according to the position of the CG and the stability of the aircraft for each static margin configuration.

Firstly, an aerodynamic model only composed of the wing, tail and rudders, is set up in XFLR5 with the origin at the LE of the wing (see Figure 35).

Following CAD specification (see Section 8.1), the main wing is constructed with a NACA 2411, but as the tail and rudders are flat plates, a symmetric NACA airfoil is used (NACA 0012) to model them.

Then, total mass (3.32kg) is shifted along the longitudinal axis to find the position of neutral point, the point at which aircraft becomes unstable if exceeded. The Simulation is computed with a fixed speed of 20m/s and same atmospheric conditions endured during the experimental flight testing.

The NP is found to be at 0.122 meters from origin. Therefore, static margin (SM) is calculated using equation 3.

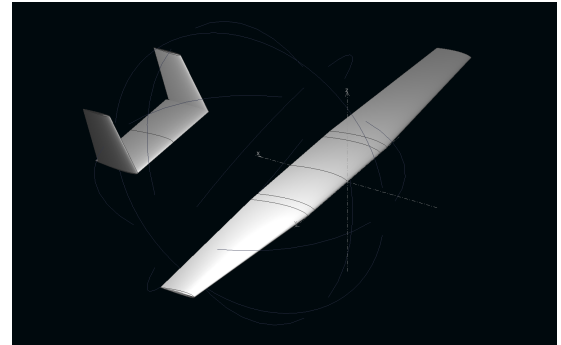


Figure 35: BUDDI model in XFLR5

$$SM = X_{NP} - X_{CG} \quad (3)$$

Then, the mass position is varied from 25% to 30% of the Mean Aerodynamic Chord (MAC = 0.176m) - which is where current CG is assumed to be - and static margin and Pitching moment against CL slopes (Figure 36) are calculated (see Table 4).

CG Position(m)	MAC(%)	Static Margin (m)	Slope
0.044	25	0.078	-0.439
0.048	27.5	0.074	-0.419
0.053	30	0.069	-0.389
0.076	43.25	0.046	-0.259
0.099	56.25	0.023	-0.124
0.122	69.3	0	0

Table 4: Extracted parameters from transition into hover

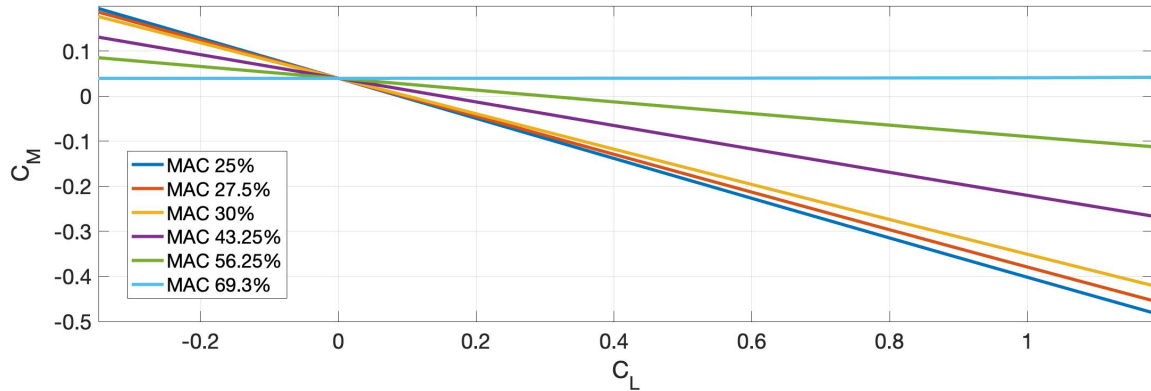


Figure 36: Pitching Moment against Lift Coefficient as CG position varies

5.3.2 Firmware

To improve BUDDI's VTOL performance, code responsible to perform the transitions is looked at in detail:

The open source firmware (written in C++) provided by Ardupilot categorizes BUDDI as QuadCopter, which is any combination of a fixed wing with a multicopter aircraft. Furthermore, it is also classified as a dual motor non-vectored tailsitter; an aircraft that rotates the fuselage when moving between forwarding flight and hover, and has a fixed rotor orientation relative to the fuselage [12].

Setting `Q_FRAME_CLASS=10` within the code defines BUDDI as a tailsitter, and allows for the sub-file within the firmware (`tailsitter.cpp`) to regulate control when it comes to transition into and out of the hover. This script mostly focuses on computing the tilt rotors output if a vectored tailsitter is given. However, in BUDDI's case, as the rotors stay fixed relative to the body, the script computes the differential throttle and elevator input.

In another firmware sub-file (`quadplane.cpp`) default flight parameters are determined.

These variables can be user-defined without actually modifying the logic of the code, which is useful as such script modifications must be tested through simulation for validation.

Key parameters to achieve a potentially improved performance are:

`Q_TAILSIT_ANGLE`: specifies how far the nose must pitch up or down before a transition in or out of the hover is complete. This means that the larger the value of the transition angle, the later the switch from one controller to the other. In BUDDI, the transition angle is set to 45 degrees.

`Q_TRANSITION_MS`: specifies a timeout for a transition from VTOL to FW flight. Even if the angle specified by `Q_TAILSIT_ANGLE` has not been reached before this interval has elapsed, the transition will be considered complete. The timeout for back transitions (from Fixed-Wing to VTOL flight) is, by default, 2 seconds.

Therefore, as an example, when transitioning to VTOL from forward-flight, active motors are switched to VTOL hover throttle, and the vehicle is pitched up toward `Q_TAILSIT_ANGLE + 5` degrees (with 55 degrees nose up being the minimum target) using the control surfaces. The transition is complete when `Q_TAILSIT_ANGLE` is reached, or when `Q_TRANSITION_MS` has elapsed. Then, Fixed-Wing controller is switch to VTOL.

In order to compensate for the increase in pitch response, suggested in section 5.3.1, both `Q_TAILSIT_ANGLE`, and `Q_TRANSITION_MS` should be reduced to match sensibility on pitch, and transition to a VTOL controller sooner. However, as mentioned above, a script simulation could be further investigated for validation purposes.

6 Conclusions

In this project, from experimental flight testing of a fixed wing drone, an analysis of its performance was carried out to generate a criterion to asses its VTOL capabilities. Then, modifications were suggested in order to improve such faculties.

The Matlab code developed and data processing for the investigation proved to be functional, as the analysis on the phases of interest successfully determined the data for future comparison with potentially improved BUDDI configurations. Besides, even though it may not contribute for the analysis, the code provided a more detailed insight for each phase through trajectory plots, and plots of airspeed, position, inertial rates, flight mode, actuators deflection and current drawn from battery with respect to time. However, for all the four interesting phases time elapsed and current consumption were extracted. Furthermore, the analysis also determined other parameters related to the flight regime such as cruise airspeed, cruise throttle and the atmospheric conditions during the experimental testing, useful for simulation purposes.

In terms of the pitch response, it could be observed that pitch matched elevator input, and the lag between actuator deflection and actual pitch proved to be relatively low. However, the new BUDDI configuration aims to increase sensitivity of pitch with respect to the elevator deflection, and reduce lag further.

The stability study in XFLR5 showed that BUDDI would be stable if CG were to be shifted backwards along the longitudinal axis up until 56.25% of MAC. This would change drastically static margin compared to where it is assumed to be (20-30% MAC). Nevertheless, the new proposed configuration is set on a more conservative position for the CG at 43.25% of the MAC. Finally, firmware modifications are proposed to enhance VTOL performance too. Both modifications are expected to decrease time elapsed and battery consumption in BUDDI - when performing the transition into the hover - to attain a more efficient and fast landing manoeuvre. However, validation is pending.

7 Future Work

The main goal of this research project is to work out the parameters which asses the performance of BUDDI for all the chosen phases, and come up with a new improved configuration based on the initial analysis. That being the case, the next natural step in this research would be to test the potentially improved BUDDI configuration and compare the data obtained from the initial's flight testing data. Further development of the code could be investigated so it automatically detects the phases of interest based on mode, pitch, airspeed and altitude.

In terms of improving the pitch response, increasing the elevator, providing BUDDI with faster actuators and reducing mass distribution are some of the modifications to be examined. However, all these modifications would also require a review on how they would affect the stability of BUDDI. Also, if the stability analysis were to be improved, a more accurate aerodynamic model of BUDDI with the included body and spars could be used.

In the long term, high precision non-linear controllers and other control approaches may be implemented to deal with the highly non-linear aerobatics endured by BUDDI. Furthermore, analogous simulation of their response could be investigated too to reduce the risk in experimental flight testing.

Ultimately, in a potential extrapolation to a wider frame context, the analysis method to determine the VTOL capabilities BUDDI could be further explored to asses such competence in other aircraft, based on static margin.

8 Appendix

8.1 BUDDI CAD Specification

BUDDI V.1				
Wing Span (mm)	1680			
Mass (g)	3320			
Fusion 360 Link	https://a360.co/37eMK2q			
Motors	AXI 2826/13			
Speed Controllers	JETI Spin66			
Props	APC 12*6			
Batteries	Quantity	Capacity (mAH)	Cells	Type
	2	4000	6	LIPO
Panel Dimensions (mm)	center Wing	Outer Wings (2 off)	Tailplane	Fins (2 off)
X Position	320	320	930	930
Span	400		430	
Semi Span		600		170
LE Sweep	0	40	0	30
Root				
Chord	200	200	150	140
Section	NACA2411-il	NACA2411-il	Flat plate	Flat plate
TE Thickness	3	3	9.525	9.525
Tip				
Tip Chord	200	120	150	95
Tip Section	NACA2411-il	NACA2411-il	Flat plate	Flat plate
TE Thickness	3	3	9.525	9.525
Control Surfaces		Ailerons (2 off)	Elevator	Rudders (2 off)
Span		570	400	150
root chord		70	80	75
tip chord		45	80	65

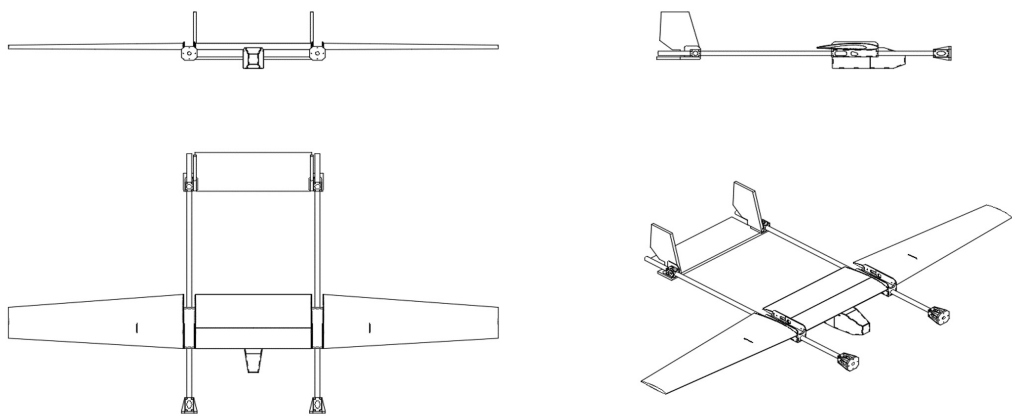


Figure 37: CAD Specification BUDDI V.1 produced by Thomas David, University of Bristol

References

- [1] T. Chang, Z. Guo, J. Zhang, and L. Wu, “Landing control scheme of vertical takeoff and landing fixed-wing uav,” in *2018 IEEE 3rd Advanced Information Technology, Electronic and Automation Control Conference (IAEAC)*, pp. 1984–1988, IEEE, 2018.
- [2] S. Huh and D. H. Shim, “A vision-based automatic landing method for fixed-wing uavs,” *Journal of Intelligent and Robotic Systems*, vol. 57, no. 1-4, p. 217, 2010.
- [3] T. Muskardin, G. Balmer, S. Wlach, K. Kondak, M. Laiacker, and A. Ollero, “Landing of a fixed-wing uav on a mobile ground vehicle,” in *2016 IEEE International Conference on Robotics and Automation (ICRA)*, pp. 1237–1242, IEEE, 2016.
- [4] P. R. Marcus Eriksson, *Launch and recovery systems for unmanned vehicles onboard ships. A study and initial concepts*. PhD thesis, KTH Royal Institute of Technology, 2013.
- [5] S. H. Mathisen, T. I. Fossen, and T. A. Johansen, “Non-linear model predictive control for guidance of a fixed-wing uav in precision deep stall landing,” in *2015 International Conference on Unmanned Aircraft Systems (ICUAS)*, pp. 356–365, IEEE, 2015.
- [6] W. Khan, *Dynamics modeling of agile fixed-wing unmanned aerial vehicles*. PhD thesis, McGill University Libraries, 2016.
- [7] W. Khan and M. Nahon, “Modeling dynamics of agile fixed-wing uavs for real-time applications,” in *2016 international conference on unmanned aircraft systems (ICUAS)*, pp. 1303–1312, IEEE, 2016.
- [8] F. M. Sobolic, *Agile flight control techniques for a fixed-wing aircraft*. PhD thesis, Massachusetts Institute of Technology, 2009.
- [9] E. Bulka and M. Nahon, “Autonomous control of agile fixed-wing uavs performing aerobatic maneuvers,” in *2017 international conference on unmanned aircraft systems (ICUAS)*, pp. 104–113, IEEE, 2017.
- [10] W. E. Green and P. Y. Oh, “A hybrid mav for ingress and egress of urban environments,” *IEEE Transactions on Robotics*, vol. 25, no. 2, pp. 253–263, 2009.
- [11] E. Bulka and M. Nahon, “Autonomous fixed-wing aerobatics: from theory to flight,” in *2018 IEEE International Conference on Robotics and Automation (ICRA)*, pp. 6573–6580, IEEE, 2018.
- [12] A. D. Team, *Tailsitter Plane - Plane documentation*, 2019 (accessed May, 2019).